Force-Free Motion of a Mercury Drop Alternatively Submitted to Shifted Asymmetric Potentials

L. Gorre-Talini, Pascal Silberzan

Force-Free Motion of a Mercury Drop Alternatively Submitted to Shifted Asymmetric Potentials

L. Gorre-Talini and P. Silberzan (*)

Laboratoire Physico-Chimie Curie (**), Institut Curie, Section de Recherche, 11 rue Pierre et Marie Curie, 75231 Paris Cedex 05, France

(Received 14 February 1996, revised 5 June 1997, accepted 24 July 1997)

PACS.05.90.+m – Other topics in statistical physics and thermodynamics
PACS.47.65.+a – Magnetohydrodynamics and electrohydrodynamics
PACS.82.45.+z – Electrochemistry and electrophoresis

Abstract. — We present a macroscopic experimental realization of force-free motion consisting in a mercury drop experiencing alternatively in time two locally asymmetric and periodic potentials which are spatially shifted. A system of electrodes creates the potentials and the force applied to the drop is of electrocapillary nature. We study the macroscopic velocity of the drop as a function of the times during which it experiences each potential and investigate different regimes of macroscopic velocity. Adjusting the different times allows some of the drops to move whereas others of different local velocities have a zero macroscopic velocity. This system thus acts as a filter. We also study the case of stochastic modulation of the potentials. These results compare well with theoretical predictions and experimentally validate a model which has been proposed for motor protein assemblies.

Résumé. — Nous présentons une réalisation expérimentale de mouvement sans force consistant à appliquer successivement à une goutte de mercure macroscopique deux potentiels localement asymétriques et périodiques, décalés dans l'espace. Chaque potentiel est créé par un système d'électrodes et la force appliquée à la goutte est d'origine électrocapillaire. Nous étudions la vitesse macroscopique de la goutte en fonction des temps d'adressage de chaque potentiel et mettons en évidence différents régimes de vitesse. Un ajustement des différents temps permet à certaines gouttes de se déplacer à vitesse finie alors que d'autres, ayant des vitesses locales différentes dans chaque potentiel, ont une vitesse macroscopique nulle. Ce système joue donc le rôle d'un filtre. Nous étudions également le cas où les systèmes d'électrodes sont adressés de façon stochastique. Les résultats confirment les prédictions théoriques et valident expérimentalement un modèle qui a été proposé pour expliquer les phénomènes mis en jeu dans le mouvement des moteurs moléculaires.

Introduction

The ability to produce a macroscopic motion without having to exert a macroscopic force or gradient (force-free motion) has been recently largely explored on the theoretical side [1–5].

(*) Author for correspondence (e-mail: Pascal.Silberzan@curie.fr)
(**) UMR CNRS/IC 168

Motivation for these studies is twofold: First, the underlying principles can help to understand how the molecular biological motors work [4, 5]. Second, they provide a template to design original separation techniques whose theoretical separation power can be astonishingly high in some cases [1, 3].

As a matter of fact, provided energy is dissipated, a particle can move over a large distance without any macroscopic force or gradient as long as the local environment the particle is submitted to is periodic and asymmetric. For instance, it has been theoretically demonstrated [1] and experimentally verified [6] that a Brownian particle submitted to such a potential successively switched on and off can experience a macroscopic drift.

In this paper, we will concentrate on the case of a particle alternatively experiencing two asymmetric potentials whose periods are identical but which are shifted by a fraction of their period.

No diffusive step is required in this model. We have chosen here to illustrate it with a macroscopic object (a 1 mm mercury drop) and therefore, temperature dependent processes such as diffusion will be ignored in the following.

The theoretical description we present thereafter is largely inspired from reference [3]. Let us first precise a few notations: we consider a particle experiencing alternatively in time the sawtooth potentials W_1 and W_2 depicted in Figure 1a. Its local mobilities in potentials W_1 and W_2 are respectively μ_1 and μ_2. The amplitudes of the potentials are respectively $\bar{W}_1$ and $\bar{W}_2$, their common period and asymmetry are respectively $p = a + b$ and a/b $(b > a)$. The two potentials are shifted by a distance δ. We note V the macroscopic velocity of the particle.

It can easily be shown by geometrical arguments that a particle experiencing successively the potential W_1 during a time τ_1 and W_2 during τ_2 can be set into a directed motion only if $a < \delta < p - a$.

When this condition is fulfilled, several velocity regimes arise depending on the values of τ_1 and τ_2 which are imposed by an external modulation (this deterministic situation will be denoted "regular case" thereafter). If $\tau_1 < ab/(\mu_1\bar{W}_1)$ or $\tau_2 < ab/(\mu_2\bar{W}_2)$, $V = 0$ since the particle does not have time to escape the energy minimum where it returns endlessly. If τ_1 and τ_2 are increased so that $\tau_i > ab/(\mu_i\bar{W}_i)$ for $i = 1$ and 2, the velocity increases to eventually reach its optimal value $p/(\tau_1 + \tau_2)$ corresponding to one period per time cycle when:

$$\mu_1\bar{W}_1\tau_1 + \mu_2\bar{W}_2\tau_2 = pb. \tag{1}$$

If τ_1 and τ_2 are further increased $V = p/(\tau_1+\tau_2)$ is still verified and the velocity thus decreases.

These different velocity regimes are summarized in the diagram of Figure 1b. In the experiments, we have chosen to fix the time τ_2 and to vary τ_1. For a given value of τ_2 different behaviours are then observed according to τ_1: if $\tau_2 < ab/(\mu_2\bar{W}_2)$ (region I, Fig. 1b), $V = 0$ whatever the value of τ_1; if $ab/(\mu_2\bar{W}_2) < \tau_2 < b^2/(\mu_2\bar{W}_2)$ (region II, Fig. 1b), three different regimes of velocity can be reached (zero velocity, intermediate velocity $0 < V < p/(\tau_1 + \tau_2)$ and optimal velocity $V = p/(\tau_1+\tau_2)$) when τ_1 is varied; if $\tau_2 > b^2/(\mu_2\bar{W}_2)$ (region III, Fig. 1b) the velocity can only be zero or optimal.

Also of interest, in particular for its possible biological relevance, is the "stochastic case" for which the particle experiences the potential W_i during a time t_i given by the probability $P(t_i) = \exp(-t_i/\tau_i)/\tau_i$. In this case, a maximum of V is also predicted although its amplitude is smaller than $p/(\tau_1 + \tau_2)$. For very small values of the average times τ_1 and τ_2, the Poisson statistics allows for long residence times with a non-zero probability. Escape from an energy minimum becomes then possible and thus V is small but finite.

We have here considered the case of a one-state particle alternatively experiencing two potentials. However, this situation is similar to a two-states particle experiencing a single external

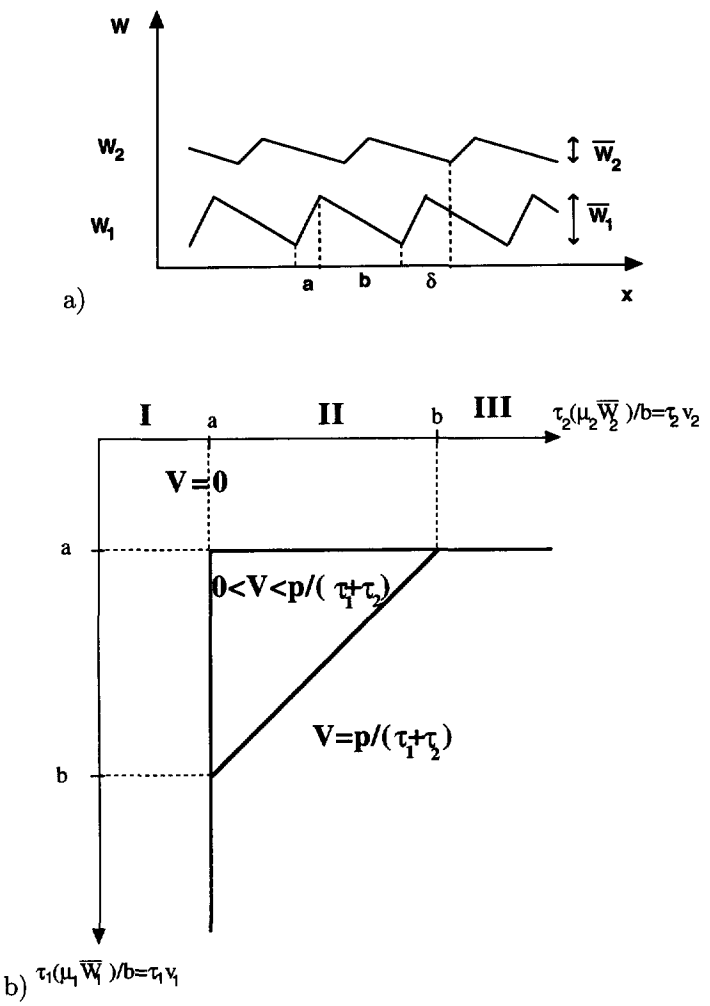

Fig. 1. — a) Schematic representation of the potentials W_1 and W_2. x is the spatial coordinate. b) Different regimes of the macroscopic velocity according to the values of $\tau_1(\mu_1\bar{W}_1)/b$ and $\tau_2(\mu_2\bar{W}_2)/b$ compared to the lengths a and b of the potentials.

potential and transiting between its two states in such a way that its energy landscape is analogous to W_1 in one of its states and to W_2 in the other.

Experimental System

In this paper, we have studied a macroscopic droplet of mercury successively exposed to potentials of electrical origin whose characteristics are similar to the ones presented in the theoretical introduction.

Mercury drops submitted to an electric field in dilute sulphuric acid move toward the cathode. This electrocapillary effect is a consequence of interfacial tension gradients on the surface of the drop (Marangoni effect) induced by the electric field. A more detailed description can be found in reference [7] and some of the characteristics of this motion will be discussed hereafter.

To produce potentials whose shapes reflect the one depicted in Figure 1a, we have used the experimental set up described in Figure 2a. A central 2 mm deep square groove is mechanically etched in a block of plexiglas. On each side of this groove, transverse pairs of grooves of 1 mm depth are also etched in a periodic way such as to be connected to the central one. All the canals are filled with 10% sulphuric acid (solutions are prepared from 95% sulphuric acid (Prolabo, France) and are used within two weeks). In each transverse canal a gold (99.99+%, Goodfellow) electrode dips in the electrolyte at a distance of about 1 cm of the central canal. The drop of mercury (99.99+%, Aldrich) is placed in the central canal and moves along it. Its diameter is larger than 1 mm in order to prevent it from entering the transverse canals.

In the following, we call "system of electrodes", all the electrodes on the same side of the central canal. By "pair of electrodes", we mean two electrodes separated by the distance a in one system of electrodes.

Each system of electrodes is addressed successively. For the system "on", a DC voltage which can be chosen different for each system is applied between the two electrodes of each pair with a double output DC generator in the range 0-30 V (Metrix). Practically, the applied voltages range from 12 V to 20 V. Taking into account the voltage drop in the transverse canal, these differences of potential correspond to effective electric fields along the central canal ranging from about 0.3 V cm^{-1} to 0.6 V cm^{-1} The commutation from one system to the other is performed *via* relays by a PC computer equipped with an I/O digital board (Keithley). The smallest commutation time that can be obtained with such a set-up is 20 ms. The experimental error on the imposed residence times is weak (about 5%).

When a DC voltage is applied between the pairs of electrodes of one system (the other system being left at a floating potential), the drop will be attracted toward the areas of the cathodes and repelled from the anodes. In Figure 2b, the energy landscape experienced by the droplet will then be similar to W_1 when the system A is addressed and to W_2 when the system B is addressed. The potentials thus produced by the pairs of electrodes on each side of the central canal have the same periodicity ($p = 25$ mm) and asymmetry ($a = 6$ mm and $b = 19$ mm) and are spatially shifted by a distance $\delta = 13$ mm. Potentials having a period of 50 mm can also be obtained by removing one pair of electrodes out of two (in this case, a and δ are unchanged and $b = 44$ mm). The total length of our set up is 50 cm which represents 20 (respectively 10) periods of the potential for each system of electrodes and for $p = 25$ mm (respectively 50 mm). The drop is observed with a CCD camera and time sequences are recorded on a VCR for further analysis.

Motion of the Drop in a DC Field

In order to quantify the velocity of the drop in each state W_i, we have characterized the motion of a drop of mercury in a DC field in our experimental set-up.

Figure 3a displays the position *versus* time plot of a drop when submitted to a field of 0.32 V cm^{-1} imposed between one of the pairs of electrodes of our set-up. As shown in this figure the motion is uniform and can thus be characterized by a velocity v. For a given drop and field, the velocity proved to be constant whatever the distance and time during which the motion was observed. Nevertheless, as shown in Figure 3b, the velocity is an increasing non linear function of the field within the applied range of field intensities.

This result differs from our previous study [8] where we had observed that the velocity of a drop in a DC field varies linearly with the intensity of the field. However, in the present study, the imposed fields are larger than in the previous one. They range from about 0.3 V cm^{-1} to 0.6 V cm^{-1} (compared to about 0.1 V cm^{-1} in Ref. [8]) and the resulting force is such that the drop goes under deformations during its motion. This velocity regime thus involves inertial

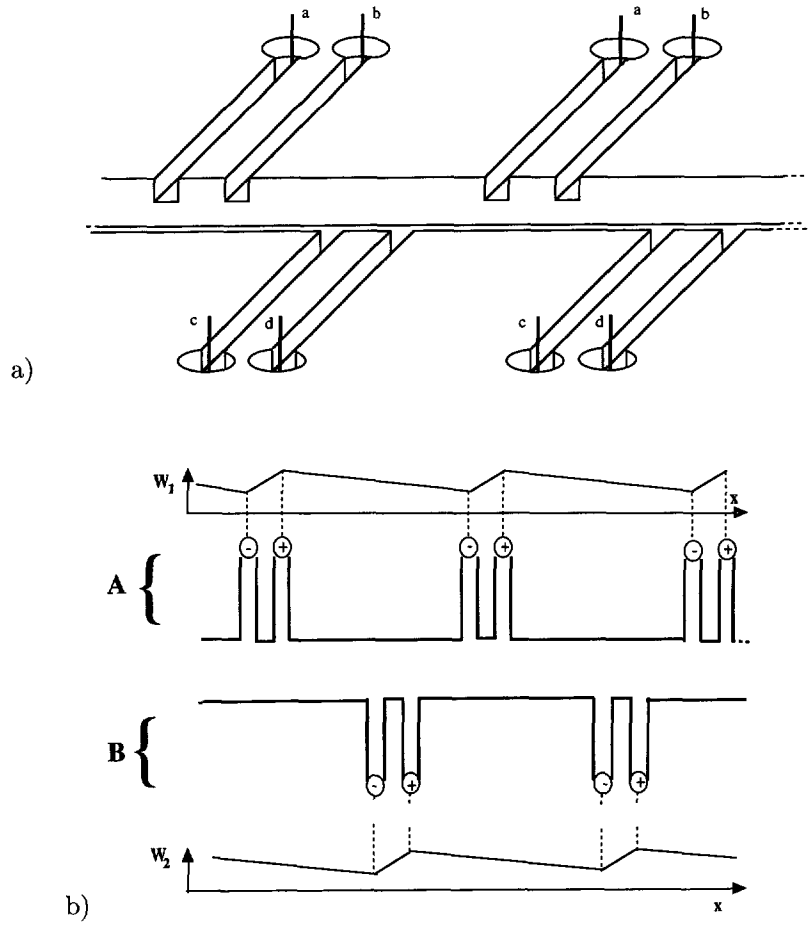

Fig. 2. — a) View of the block of plexiglas. The central canal is 2 mm deep and 2 mm wide and the transverse ones are 1 mm deep and 1 mm wide. The electrodes dip in the electrolyte which entirely fills the canals. The electrodes a (respectively b, c, d) are interconnected. An experiment proceeds as follows: one of the systems of electrodes (for instance the system formed by the electrodes a and b) is first addressed which consists in imposing a difference of potential corresponding to $\bar{W}_1$ between electrodes a and b during a time τ_1. The electrodes of the other system (c and d) are then left at a floating potential. We then switch to the other system by imposing a difference of potential corresponding to $\bar{W}_2$ between the electrodes c and d during a time τ_2, the electrodes a and b being left at a floating potential. We then address the first system again and so forth... b) Schematic top view of the experimental set-up and approximate shapes of the potentials created by each system of electrodes along the central canal. The two systems are addressed successively. W_1 corresponds to system A when system B is floating, W_2 to system B when system A is floating.

effects and, to our knowledge, has never been studied in detail. However, as shown in [7], one can get a qualitative picture of the phenomenon by equating the driving electric force and the dynamic pressure (Bernoulli's law). In this approximation, the viscous drag is neglected and one gets for the velocity:

$$v \propto \sqrt{\mathcal{E}} \tag{2}$$

where $\mathcal{E}$ is the electric field.

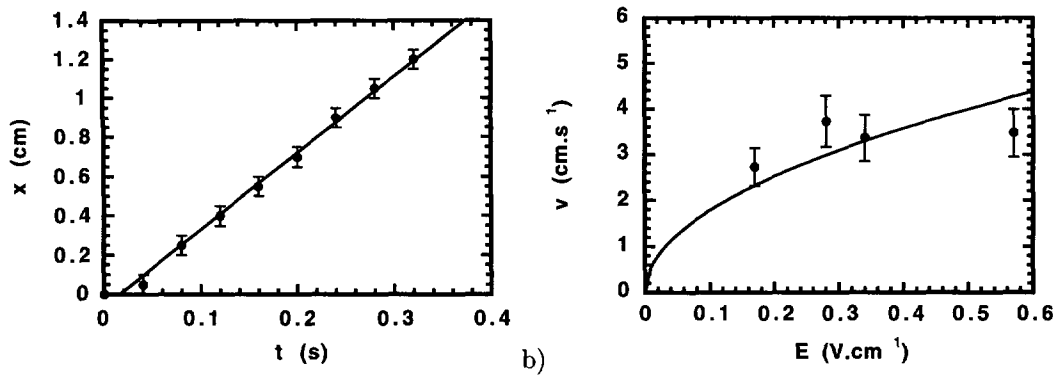

Fig. 3. — a) Position of a drop of mercury as a function of time in a dc field of 0.32 V cm^{-1}. b) Velocity of a drop of 1.9 mm diameter as a function of the electric field. The solid line is fitted to the data following equation (2).

As shown in Figure 3b, our experimental data seem to roughly fit this law. To compare our results with the theoretical predictions of reference [3], we have systematically measured the local velocities ν_1 and ν_2 in potentials W_1 and W_2 for each drop. Besides, a mobility cannot be strictly defined in each potential as $\mu_i = \nu_i b/\bar{W}_i$ would be a function of the potential amplitude $\bar{W}_i$ and in the following we have replaced the expression $\mu_i \bar{W}_i/b$ by the velocity ν_i over the length b of the potential W_i (the different threshold times do not depend on the local velocities over the length a of each potential). In the following, we will refer to the electrocapillary velocities ν_i as the "local" velocities which are to be distinguished from the macroscopic velocity V of the drop resulting from several transitions between the two systems of electrodes.

Experimental Results

REGULAR CASE. — We have first studied the motion of the drop for different values of τ_1 and τ_2 imposed in the regular case. Figure 4a shows a typical position *versus* time plot when τ_1 and τ_2 are long enough to enable the drop to move a distance $p = a + b$ every time cycle. The macroscopic velocity V is thus $p/(\tau_1 + \tau_2)$. Figure 4b shows an example of motion for intermediate values of τ_1 and τ_2. Several time cycles are then needed for the drop to move a distance p as local backward motion occurs.

The macroscopic velocity of the drop is obtained by analysing the recorded sequences of motion. When the drop is in a regime where it regularly moves a distance p every time cycle, its velocity is given by $p/(\tau_1+\tau_2)$. Hence there is no measurement error in the regime of optimal velocity. When the motion of the drop is more complex (such as in Fig. 4b) the velocity is obtained by measuring the time needed for the drop to move along the length of the central canal which represents 20 periods of each potential. In this regime, the vertical error bars represent the measurement errors.

Figure 5a shows two plots of the normalized velocity $V^*(\tau_1+\tau_2)/p$ as a function of τ_1 for two fixed residence times τ_2 in state W_2. In order to explore the diagram depicted in Figure 1b, we have investigated several regimes. We have taken three fixed values of $\nu_2\tau_2$ in the three regions of Figure 1b: $\nu_2\tau_2 < a$, $a < \nu_2\tau_2 < b$ and $\nu_2\tau_2 > b$.

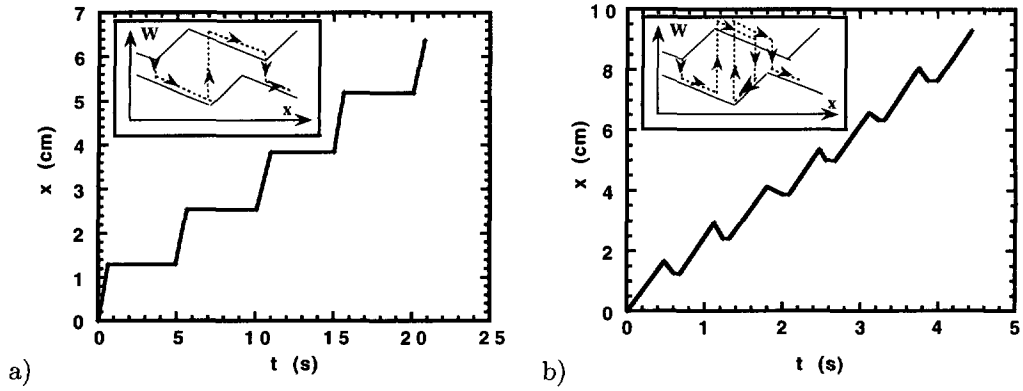

Fig. 4. — Position of a drop of diameter 1.6 mm as a function of time for a difference of potential of 0.65 V in the central canal for both systems of electrodes. a): $\tau_1 = \tau_2 = 0.2$ s, b): $\tau_1 = \tau_2 = 5$ s. Inserts: time sequences experienced by the droplet.

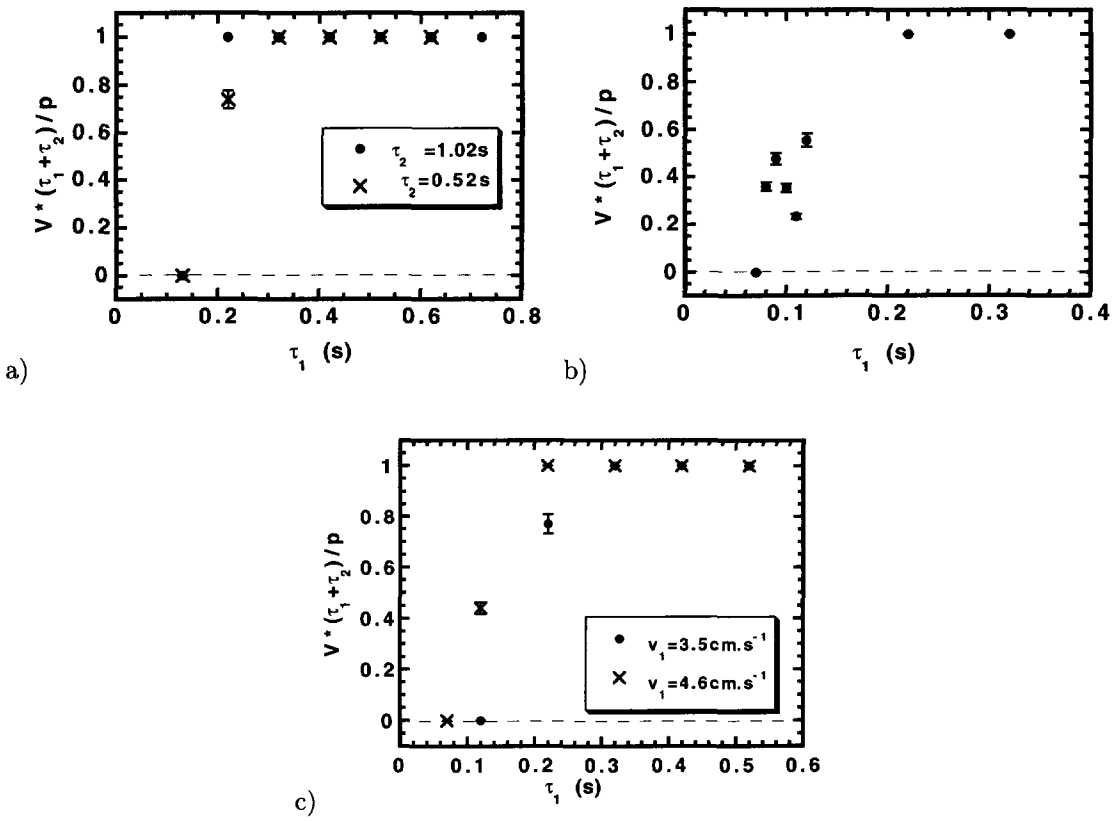

Fig. 5. — Normalized velocity $V^*(\tau_1+\tau_2)/p$ as a function of τ_1 in the regular case. a) Plots for a drop of diameter 1.9 mm for two different times τ_2. The local velocities in each state W_i are respectively: $\nu_1 = 4.0$ cm s^{-1} and $\nu_2 = 3.5$ cm s^{-1} b) Three velocity regimes for a drop of velocities $\nu_1 = 8.1$ cm s^{-1} and $\nu_2 = 4.1$ cm s^{-1}. c) Plots for a drop having different local velocities in state W_1. This situation is equivalent as two drops of different mobilities in the same set-up.

In each case, we have made $\nu_1\tau_1$ vary and we have measured the macroscopic velocity. Practically, we have here $\nu_2 = 3.4$ cm s^{-1} and $\nu_1 = 4$ cm s^{-1}

1. If $\tau_2 = 0.1$ s then $\nu_2\tau_2 < a$ and we have verified that $V = 0$.

2. If $\tau_2 = 0.52$ s (Fig. 5a, stars) we are then in the case where $a < \nu_2\tau_2 < b$. According to the value of τ_1 we then observe several different regimes:

   2.1 if $\tau_1 \leq 0.12$ s then $V = 0$ (region I, Fig. 1b),

   2.2 if $\tau_1 = 0.22$ s we are in a situation where the velocity is finite but slightly smaller than the optimal velocity ($V \approx 0.8\ p/(\tau_1 + \tau_2)$),

   2.3 if $\tau_1 \geq 0.24$ s, the optimal velocity is reached: $V = p/(\tau_1 + \tau_2)$.

We have thus observed the three regimes predicted in that situation (region II, Fig. 1b).

From the basic equations we can calculate the two threshold times. The transition from $V = 0$ to intermediate velocity is expected when $\tau_1 = \bar{\tau}_1 = a/\nu_1$, the other transition from intermediate velocity to optimal velocity is expected at $\tau_1 = \tau_1^* = (p - \nu_2\tau_2)/\nu_1$. Numerically, we get $\bar{\tau}_1 = 0.15 \pm 0.02$ s and $\tau_1^* = 0.18 \pm 0.04$ s both values being compatible with the measured threshold times.

3. In this last case, $\tau_2 = 1.02$ s (Fig. 5a, dots).

We observe only two regimes, $V = 0$ or $V = p/(\tau_1 + \tau_2)$ and we have not succeeded in identifying a third one of intermediary velocity. Again this result is in accordance with theoretical predictions (region III of Fig. 1b). The value of the threshold time is the same as in the preceding case: $\bar{\tau}_1 = 0.15$ s and is compatible with our observations.

We have thus observed the different velocity regimes predicted by theory. In particular, we have shown that adjusting one of the times leads to very different behaviours: in one case only two values of the normalized velocity of the drop (0 or 1) are allowed whereas in the other case intermediate values can be reached.

Figure 5b more accurately describes the three velocity regimes that occur when $\nu_2\tau_2 < b$. The calculated values of $\bar{\tau}_1$ and τ_1^* are respectively 0.07 ± 0.01 s and 0.10 ± 0.03 s. In that case we have investigated the variations of the velocity in the intermediate regime which experimentally occurs for $0.08 \leq \tau_1 \leq 0.12$ s. In this regime, the velocity exhibits irregular variations. As the velocity should be an increasing function of the time τ_1 in this regime, this behaviour probably mirrors both the influence of small variations of the lengths a and b of the potentials (due to the finite width of the lateral canals) and the fact that the velocity is averaged over a restricted number of periods. The high sensitivity of the velocity to these features of the potentials may also be revealing of a complex dependence of V *versus* τ_1 in this regime. However, the lack of sensitivity of our set up has prevented us from further studying these variations. Nevertheless, if τ_1 is long enough (*i.e.* is not too close to the threshold value $\bar{\tau}_1$) this influence disappears and the velocity regularly increases with τ_1 in this regime.

In order to check the influence of the mobility in each potential on the velocity, we have taken advantage of the non linear behaviour of the local velocity when the electric field varies. In Figure 5c are displayed the normalized $V(\tau_1)$ curves of the same drop submitted to two different potential amplitudes $\bar{W}_1$. The amplitude $\bar{W}_2$ and thus the local velocity ν_2 is the same for both curves and is such that the drop moves a distance $\nu_2\tau_2 < b$ in state $\bar{W}_2$. The amplitudes $\bar{W}_1$ and thus the local velocities ν_1 differ: $\nu_1 = 3.5$ cm s^{-1} (Fig. 5c, dots) and $\nu_1 = 4.6$ cm s^{-1} (Fig. 5c, stars). Although these results are obtained with the same drop

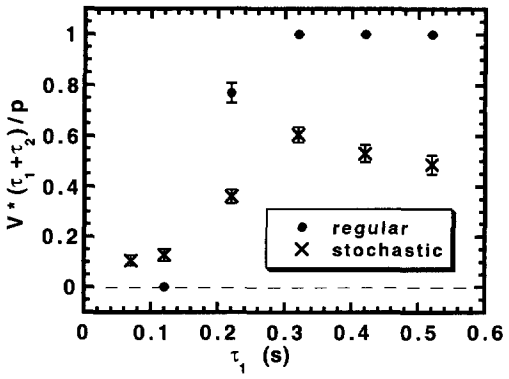

Fig. 6. — Normalised velocity $V^*(\tau_1 + \tau_2)/p$ of a drop of diameter 1.9 mm as a function of τ_1 in the stochastic and regular cases. $\nu_1 = 3.5$ cm s^{-1} and $\nu_2 = 3.4$ cm s^{-1}

they mimic the behaviour of two different objects submitted to the same potentials and having different mobilities.

Because of the different local velocities, the calculated threshold times are different (respectively $\bar{\tau}_1 = 0.17 \pm 0.03$ s and $\bar{\tau}_1 = 0.13 \pm 0.02$ s). At $\tau_1 = 0.12$ s, the drop whose velocity ν_1 is the smallest has a zero velocity whereas the other drop moves almost a half period during a time cycle. The system thus acts as a filter whose characteristics are fully controlled by the operator just by changing a residence time or the amplitudes of the potentials.

Of course, as our set-up is one-dimensional, this "filter effect" cannot be directly observed but these observations suggest that the transposition of such a device to microscopic scales may result in highly effective adjustable filters and therefore to powerful separation techniques.

STOCHASTIC CASE. — As we have investigated the behaviour of a drop in the regular case, we have also studied the $V(\tau_1)$ curves in the stochastic case. In this case, the potential W_i is experienced during a time t_i occurring with the probability $P(t_i) = \exp(-t_i/\tau_i)/\tau_i$ for given times τ_1 and τ_2. As pointed out in reference [3], the interest of the stochastic case is that it could provide a paradigm for motor protein assemblies. Moreover, among all the models of force free motion, the case of shifted potentials seems to be the more appropriate to describe the motion of motor proteins [9].

As shown in reference [9], in the stochastic case the displacement can be analytically calculated for each times τ_1 and τ_2 and a given set of parameters. We are therefore able to compare our results with the calculated expression of the velocity using the same set of parameters as in the real experiment.

As for the experimental values of the velocity, the problem is to measure the velocity of the drops with good enough precision. Averaging the motion over different runs is not enough, the number of needed runs being too large. To improve the statistics, we cut each trajectory into shorter ones whose duration is the average time τ_2. We thus obtain about 100 displacements that we average. As the times are stochastic, these displacements are independent from each other. We repeat the process for trajectories of duration $2\tau_2$, $3\tau_2$ *etc.* [10]. We plot these average displacements as a function of time and the average velocity is then the mean slope of this curve.

Figure 6 displays the plot of the normalized velocity $V^*(\tau_1+\tau_2)/p$ as a function of τ_1 of a drop in a given potential geometry and for both the regular and stochastic case. The vertical error

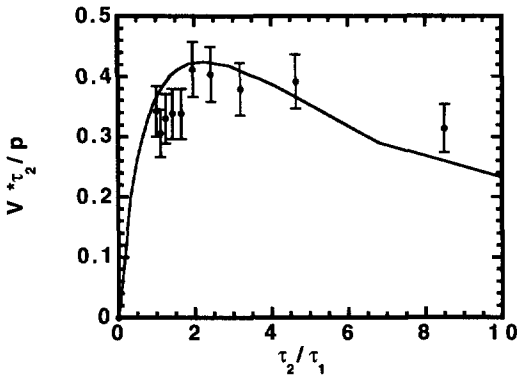

Fig. 7. — $V^*\tau_2/p$ as a function of τ_2/τ_1 in the stochastic case. The experimental results (circles) and the theoretical values (solid line) correspond to the same parameters. $a = 6$ mm, $\delta = 12$ mm, $p = 25$ mm, $\nu_1 = 4.0$ cm s^{-1} and $\nu_2 = 3.5$ cm s^{-1}

bars on the curve corresponding to the stochastic case represent the statistical uncertainty. The distance $\nu_2\tau_2$ is smaller than b. Compared to the regular case, curves in the stochastic case are smoothed out. When $\tau_1 \leq \bar{\tau}_1 = 0.17 \pm 0.03$ s, the zero velocity regime is no longer observed as the velocity is weak (at $\tau_1 = 0.07$ s, the drop moves about $0.1p$ per time cycle) but finite. The optimal velocity is reached for the same time $\tau_1 = 0.32$ s but is smaller than in the regular case. The drop actually moves about $0.6p$ instead of one period during a time cycle.

We have not systematically investigated the influence of the mobility as the stochastic case is not adapted to separation purposes. Indeed, unlike in the regular case, no filter function can be achieved in this stochastic case since there is no zero velocity regime. Besides contrasts between velocities of different particles are expected to be much weaker.

In Figure 7, we have compared experimental results (dots) in another stochastic case with theoretical expression of the velocity (solid line). As in reference [3], we have plotted the normalized velocity $V^*\tau_2/p$ as a function of the stimulation rate τ_2/τ_1 between potentials 1 and 2. The agreement between theory and experiment is very good. Here, we have used the experimental values of p, ν_1 and ν_2.

Although the agreement is not always as quantitative, qualitatively the main features of the experiments are well described by theory.

Conclusion

In conclusion, we have investigated the behaviour of a droplet of mercury submitted alternatively in time to two periodic and locally asymmetric potentials spatially shifted. We have identified the regimes of macroscopic velocity predicted by theory in the regular and stochastic cases. In particular, in the regular case, a maximal velocity $V = p/(\tau_1 + \tau_2)$ can be obtained by correctly adjusting the residence times in the potentials provided the condition $a < \delta < p - a$ is fulfilled. Moreover we have verified that if the drop experiences one of the potentials during a time shorter than a threshold value, the macroscopic velocity is strictly zero. The threshold times between the different observed regimes not only depend on the characteristic lengths of the potentials but also on the local velocities of the particles in the potentials. The system thus acts as a filter selecting particles according to their local velocities in the potentials. The potentiality of such a system in the field of separation techniques thus clearly appears,

as it could provide not only high velocities of separations but also strong resolutions due to this "filter effect". In the stochastic case, the experimental values of the velocity are in good agreement with the theory. In particular, the velocity is finite for small residence times and presents an optimal value smaller than in the regular case.

Acknowledgments

We thank J. Prost, A. Ajdari and J.F. Chauwin for fruitful discussions.

References

[1] Ajdari A. and Prost J., *C. R. Acad. Sci. Paris Série II* **315** (1992) 1635; Ajdari A., Lewiner J., Prost J. and Viovy J.L., U.S. Patent No 5593565 (1997).
[2] Prost J., Chauwin J.F., Peliti L. and Ajdari A., *Phys. Rev. Lett.* **72** (1994) 2652; Peskin C.S., Ermentrout G.B. and Oster G.F., in "Cell mechanics and cellular engineering", V.C. Mow *et al.* Eds. (Springer Verlag, N.Y., 1994).
[3] Chauwin J.F., Ajdari A. and Prost J., *Europhys. Lett.* **27** (1994) 421.
[4] Astumian R.D. and Bier M., *Phys. Rev. Lett.* **72** (1994) 1766; Astumian R.D., *Science* **276** (1997) 917.
[5] Vale R.D. and Oosawa F., *Adv. Biophys.* **26** (1990) 97.
[6] Rousselet J., Salomé L., Ajdari A. and Prost J., *Nature* **370** (1994) 446; Faucheux L., Bourdieu L., Kaplan P. and Libchaber A., *Phys. Rev. Lett.* **74** (1995) 1504; Faucheux L. and Libchaber A., *J. Chem. Soc. Faraday Trans.* **91** (1995) 3163-3166; Gorre-Talini L., Jeanjean S. and Silberzan P., *Phys. Rev. E* **56** (1997) 2025.
[7] Levich in Physico-chemical hydrodynamics (Prentice Hall, Englewood, 1962).
[8] Gorre L., Ioannidis E. and Silberzan P., *Europhys. Lett.* **33** (1996) 267.
[9] Chauwin J.F., Ph.D. Thesis, Université Paris VI, France (1995).
[10] Faucheux L.P., Ph.D. dissertation, Princeton University (1995).